博士論文（要約）

Dynamic and Viscoelastic Behavior of

Discontinuous Carbon Fiber Reinforced

Thermoplastics

（不連続炭素繊維強化熱可塑性樹脂複合材料の

動的特性および粘弾性に関する研究）

呂　秀啓

Dynamic and Viscoelastic Behavior of Discontinuous Carbon Fiber Reinforced Thermoplastics

不連続炭素繊維強化熱可塑性樹脂複合材料の動的特性および粘弾性に関する研究

東京大学大学院工学系研究科システム創成学専攻
37-137251　呂秀啓
指導教員　髙橋 淳 教授

Key Words: CFRTP, Elastic modulus, Tape length, Temperature dependence, Vibration

1. Introduction

Nowadays, carbon fiber reinforced plastics (CFRP) are earning high popularity in automotive industry. Continuous CFRP have already been widely applied in loading-bearing structures of airplane. Discontinuous CFRP are developed to manufacture structures of volume-production automobile on account of their remarkable process flowability.

CFRP could be divided into carbon fiber reinforced thermosetting resin (CFRTS) and carbon fiber reinforced thermoplastics (CFRTP). Unlike thermosetting resins which remain in permanent solid state once cured, thermoplastics could be melted into liquid state and cooled back into solid state cyclically. CFRTP become more prevalent in automobile industry owing to their excellent recyclability and shorter manufacturing cycles [1]. Chopped carbon fiber tape reinforced thermoplastics (CTT) and carbon fiber mat reinforced thermoplastics (CMT) are in-plane isotropic composites being developed to manufacture mass-production vehicles [2].

Compared to CFRTS with cross-linked molecular chains in 3D space, CFRTP present noticeable viscoelastic properties because of their linear molecular chains without chemically bonds. Considerable experimental and theoretical research about time and temperature dependent mechanical properties has been focused on continuous CFRP [3-6]. Modulus of CFRTP varied remarkably at dissimilar strain sates and temperatures. In case of CTT with different tape lengths, they present different temperature dependence. This viscoelastic phenomenon was investigated primarily by using micromechanics of discontinuous carbon fiber reinforced plastics composite.

Due to the weak reinforcement along the thickness direction of CMT or CTT, the transversal shear effect has a significant influence on flexural deformation. The transversal shear modulus and flexural modulus could be determined by vibration test [7-12]. In this study, Timoshenko beam theory combined with an iterative algorithm was employed to determine the flexural and transverse shear moduli.

Voids, resin-rich region, cracks, delamination are common flaws inside of CFRP. Peter Cawley [13] proposed simplified defect models to verify the applicability to inspect CFRP parts. In this study, one modified mathematic expression was derived to evaluate the health condition of CFRTP materials and structures.

2. Materials

Two types of modified thermoplastics were used as matrix, i.e., polypropylene (PP) and polyamide 6 (PA6). CMT materials were provided by Toray Industries, Inc.. CTT materials were offered by Industrial Technology Center of Fukui Prefecture. Innumerable discontinuous fibers (6 mm in length) were dispersed randomly within in a plane (see Fig. 1). The unidirectional prepreg tapes were distributed randomly in a plane. The local representative volume element (RVE) with the stacking unidirectional prepreg tapes is more like a quasi-isotropic continuous fiber reinforced laminate (see Fig. 2).
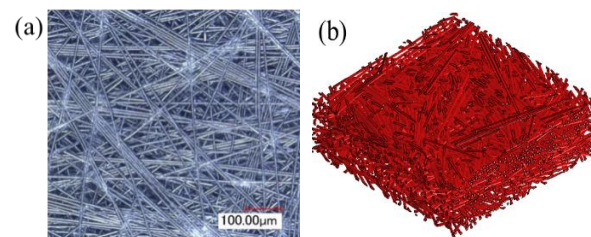

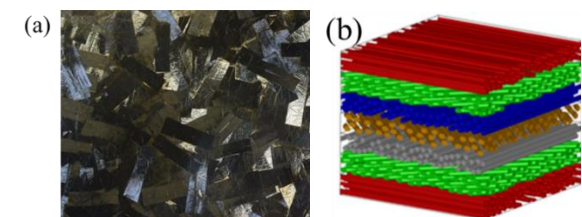Fig. 1. CMT: (a) surface observation; (b) schematic of meso-level structure.

Fig. 2. CTT: (a) surface observation; (b) schematic of meso-level structure.

3. Viscoelastic behavior

3.1 Temperature dependence

There is no chemical bonds between linear thermoplastic molecular chains, which contributed to the viscoelastic properties of CFRTP. The temperature dependence of CTT could be seen clearly from Fig. 3.
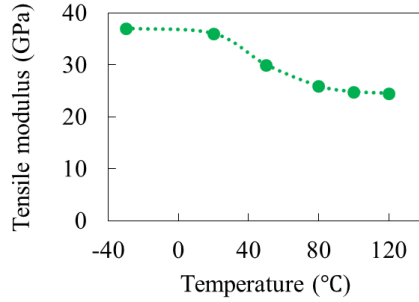

Fig. 3. Temperature dependence of CTT (6 mm).

3.2 Strain rate dependence

CMT and CTT exhibit marked viscoelasticity (see Figs. 4) when undergoing deformation. Both CMT (Vf 20%) and CTT (18 mm) present excellent log-linear relationship between modulus and strain rate.
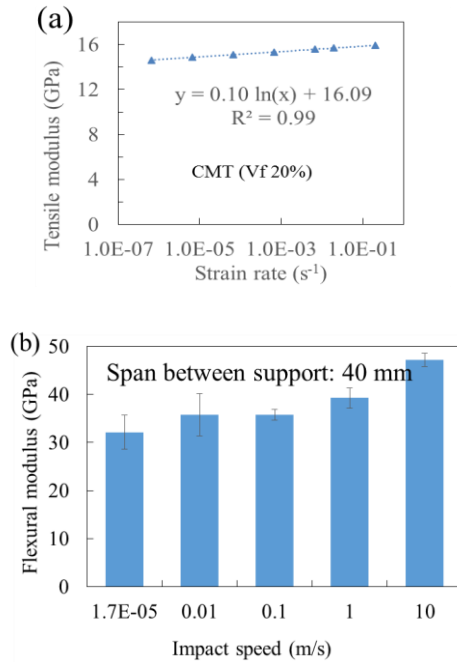

Fig. 4. Strain rate dependence: (a) CMT; (b) CTT;

3.3 Tape length dependence

The reinforcement of tapes with different lengths are different. As shown in Figs. 5 and 6, the tape length has significant influence on the mechanical properties of CTT. In order to explore the effect of tape aspect

ratio on mechanical properties, the influence of fiber aspect ratio (L/d) was analyzed (see Fig. 7).
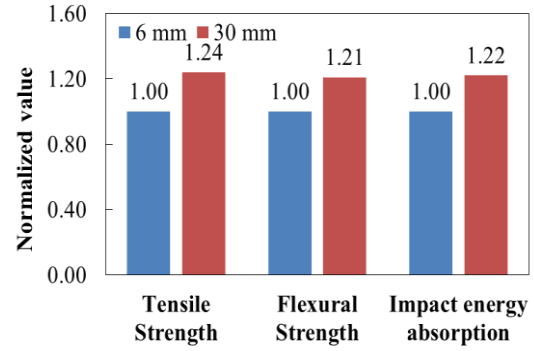

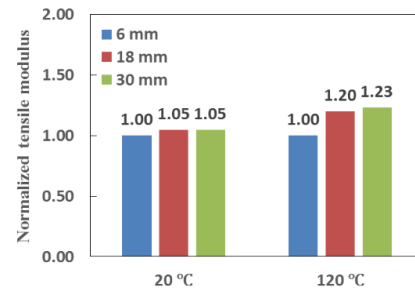Fig. 5. Tape length dependence.

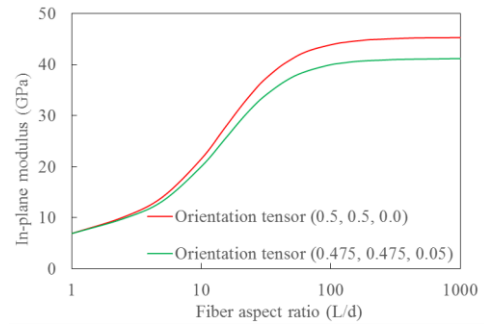

Fig. 6. Temperature dependence of modulus.

Fig. 7. Aspect ratio dependence of discontinuous fiber reinforced plastics.

As shown in Fig. 8, one innovative method was proposed to describe the aspect ratio of tape, and the corresponding aspect ratio of fiber was derived according to the volume equivalence principle. The process of derivation was listed in Eqs. (1) - (5) below.
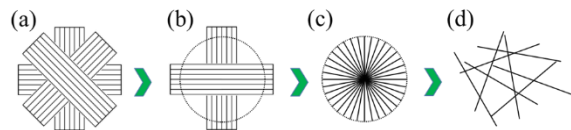

Fig. 8. Schematic of equivalent aspect ratio: (a) quasi-isotropic element; (b) two binding tapes; (c)

equivalent intermedia; (d) randomly orientated fibers.

$$V_t = 2L_t * W_t * t \qquad (1)$$

$$V_{int.} = \pi L^2 * 2t \qquad (2)$$

According to the volume equivalence principle

$$V_t = V_{int.} \qquad (3)$$

$$\left(\frac{L}{d}\right)_{int.} = \frac{1}{\sqrt{\pi}}\left(\frac{\sqrt{L_t * W_t}}{d}\right) \qquad (4)$$

$$\left(\frac{L}{d}\right) = k\left(\frac{L}{d}\right)_{int.} \qquad (5)$$

where,

L_t= length of the tape

W_t= width of the tape

t= thickness of the tape

L = length of the fiber

k= curve-fitting parameter

d= diameter of the fiber

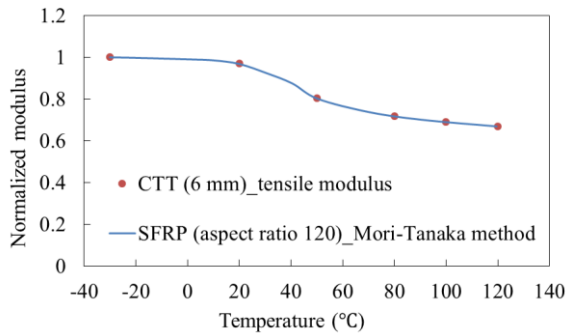$V_{int.}$= volume of the intermedia

V_t= volume of the tape

Fig. 9. Equivalent aspect ratio for CTT (6 mm).

The curve-fitting parameter (k= 0.27) was obtained from the Fig. 9. Therefore, the aspect ratio correspondence between fiber and tape was calculated (see Table 1).

Table 1. The aspect ratio correspondence between fiber and tape.

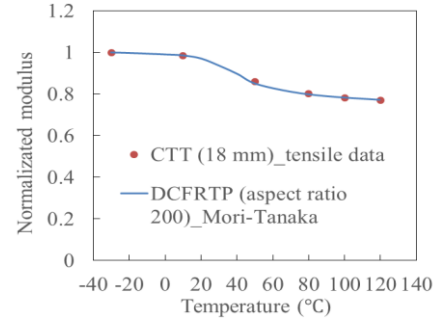| Tape length (mm)	6.0	18.0	30.0
Tape thickness (mm)	0.044	0.044	0.044
Tape width (mm)	5.0	5.0	5.0
Diameter of fiber (mm)	0.007	0.007	0.007
Equivalent aspect ratio of fiber	120	200	260

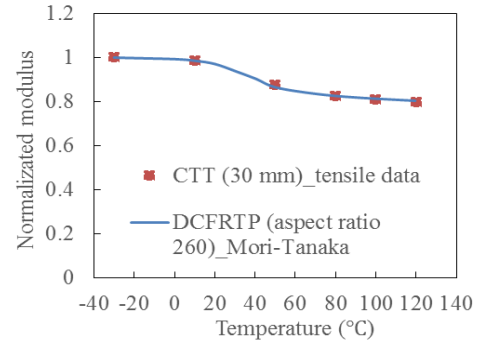Fig. 10. Equivalent aspect ratio for CTT (18 mm).

Fig. 11. Equivalent aspect ratio for CTT (30 mm).

The validation was verified by the Figs. 10 and 11. By means of micromechanics (Mori-Tanaka method), the effective modulus of CTT was obtained by calculating modulus of randomly 2D short fiber reinforced plastics (SFRP).

4. Determination of moduli by vibration

Timoshenko beam equation was proposed to analyze effects of shear deformation during flexural vibration. Flexural modulus E and transversal shear modulus G were obtained as illustrated in Figs. 12 and 13.
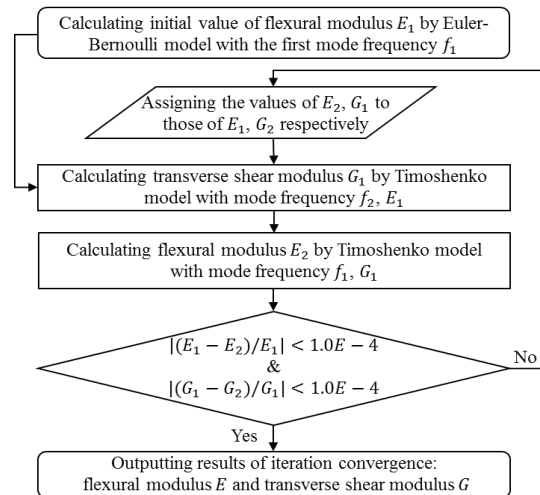

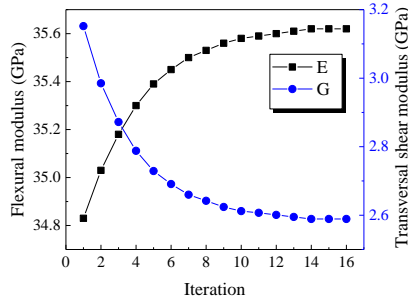Fig. 12. Flow diagram of the moduli calculation.

Fig. 13. Loop iterations of moduli calculation.

Table 2. Sets of (G_j, E_i) obtained from different combinations of eigenfrequencies.

		frequencies used to calculate E					
		f_1	f_2	f_3	f_4	f_5	f_6
Frequencies used to calculate modulus G	f_2	(G_2, E_1)					
	f_3	(G_3, E_1)	(G_3, E_2)				
	f_4	(G_4, E_1)	(G_4, E_2)	(G_4, E_3)			
	f_5	(G_5, E_1)	(G_5, E_2)	(G_5, E_3)	(G_5, E_4)		
	f_6	(G_6, E_1)	(G_6, E_2)	(G_6, E_3)	(G_6, E_4)	(G_6, E_5)	
	f_7	(G_7, E_1)	(G_7, E_2)	(G_7, E_3)	(G_7, E_4)	(G_7, E_5)	(G_7, E_6)

As shown in Table 2, sets of (G_j, E_i) were calculated accurately by combining any two of the eigenfrequencies. These sets of moduli were within certain small ranges, as listed in the following expression:

$$min(G_i) \leq G \leq \ max(G_i)$$
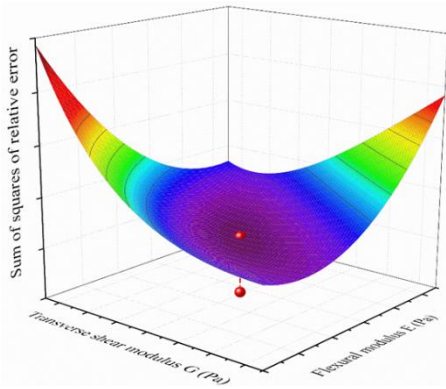$$min(E_i) \leq E \leq \ max(E_i)$$

(6)

Fig. 14. Accurate determination of transverse shear and flexural moduli.

As shown in Fig. 14, the set of moduli (G, E) were obtained by choosing the lowest sum of squared relative difference between the first seven measured frequencies and the corresponding calculated eigenfrequencies.
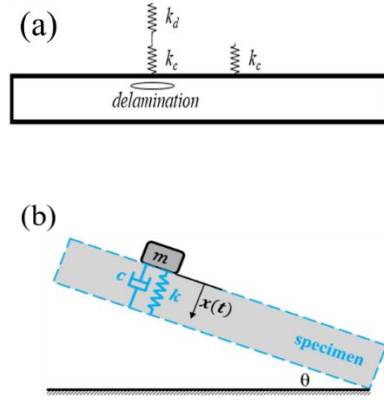
5. Nondestructive inspection by tapping

Fig. 15. Simplified defect model: (a) schematic of tapping inspection; (b) DSHM model.

The detection mechanism of local method was illustrated in Fig. 15 (a). Stiffness k_d in the delaminated area was significantly lower than stiffness k_c in the sound area. The damped simple harmonic motion (DSHM) system (see Fig. 15 (b)) was adopted to describe inspection behaviour. m is mass of the hammer, c is damping of the local tapping point, k is the measured stiffness, x(t) is displacement of the hammer, θ is angle between horizontal plane and tapping surface.
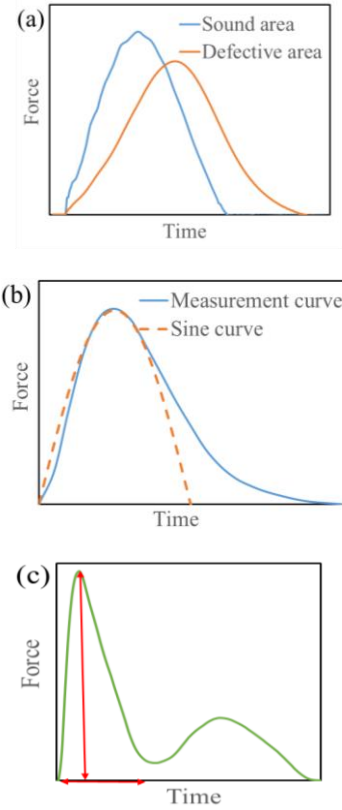

Fig. 16. Interactive force-time curve analysis: (a) comparison of force-time curves; (b) characteristic of force-time curve; (c) common force-time curve.

4

In order to simplify theoretical analysis, curve of force-time was viewed as strict sine curve. Eqs. (7) and (8) were obtained to express contact duration t_c and force amplitude $f_{\max}$.

$$t_c = \pi \sqrt{\frac{m}{k}} \tag{7}$$

$$f_{\max} = \sqrt{km} v_0 \tag{8}$$

where v_0 is initial velocity of hammer. The Force-Time curve is effected significantly by the structures' constraint, and is not strict Sine curve. Additionally, it is often difficult to measure the contact time owing to the un-closed Force-Time curve with time axis. Therefore, the peak of interactive force profile would be regarded as a significant alternative and an accurate parameter to identify defect when tapping velocities were fixed.

6. Conclusions

The critical length of tape increased with elevating temperature due to the reduction of shear strength between fiber and matrix. Both CMT and CTT present excellent log-linear relationship between modulus and strain rate.

Under room temperature, the critical length of tape is a little longer than 6 mm with respect to the modulus, while the critical length of tape is much longer than 6 mm in case of strength and impact energy absorption of CTT laminate. An innovative method was proposed to describe the aspect ratio of tape, and the corresponding aspect ratio of fiber was adopted to calculate the effective modulus of CTT using Mori-Tanaka method.

Timoshenko beam theory was combined with an iterative algorithm to calculate the moduli. Meanwhile, the least square method was employed to precisely locate the optimized moduli by fitting the measured frequencies and the calculated frequencies.

One smart tapping system was designed to analyse the feasibility to detect defects. The peak of interactive force profile was derived theoretically. This parameter would be regarded as a significant alternative and an accurate parameter to identify defect when tapping velocities were fixed.

Acknowledgements

References

[1] J. Takahashi, Development of innovative CFRTP technologies for mass-produced cars, JEC Compos. Mag. (2013) 44–45.

[2] J. Takahashi, Japanese challenge in carbon fiber composites for mass production automotive application, in: 1st Int. Symp. Emerg. Funct. Mater., 2015.

[3] C. Elanchezhian, B.V. Ramnath, J. Hemalatha, Mechanical Behaviour of Glass and Carbon Fibre Reinforced Composites at Varying Strain Rates and Temperatures, Procedia Mater. Sci. 6 (2014) 1405–1418.

[4] M. Miwa, N. Horiba, Strain rate and temperature dependence of tensile strength for carbon/glass fibre hybrid composites, J. Mater. Sci. 28 (1993) 6741–6747.

[5] T. Peijs, E. Smets, L. Govaert, Strain rate and temperature effects on energy absorption of polyethylene fibres and composites, Appl. Compos. Mater. 1 (1994) 35–54.

[6] M. Nakada, Y. Miyano, M. Kinoshita, R. Koga, T. Okuya, R. Muki, Time-Temperature Dependence of Tensile Strength of Unidirectional CFRP, J. Compos. Mater. 36 (2002) 2567–2581.

[7] Lubarda V, Chen M. On the elastic moduli and compliances of transversely isotropic and orthotropic materials. J Mech Mater Struct 2008;3:153–71.

[8] Adams RD, Maheri MR. Dynamic flexural properties of anisotropic fibrous composite beams. Compos Sci Technol 1994;50:497–514.

[9] Tolf G, Clarin P. Comparison between flexural and tensile modulus of fibre composites. Fibre Sci Technol 1984;21:319–26.

[10] Ip KH, Tse PC. Determination of Dynamic Flexural andShear Moduli of Thick CompositeBeams Using Natural Frequencies. J Compos Mater 2001;35:1553–69.

[11] Larsson P-O. Determination of young's and shear moduli from flexural vibrations of beams. J Sound Vib 1991;146:111–23.

[12] Ip KH, Tse PC. Determination of Dynamic Flexural andShear Moduli of Thick CompositeBeams Using Natural Frequencies. J Compos Mater 2001;35:1553–69.

[13] P. Cawley, R.D. Adams, A Vibration Technique for Non-Destructive Testing of Fibre Composite Structures, Journal of Composite Materials 13 (1979) 161–175.